Novel Integrated Fluid-Power Actuators for Functional End-Use Components and Systems via Selective Laser Sintering Nylon 12

Jonathon E. Slightam & Vito R. Gervasi

Rapid Prototyping Research, Milwaukee School of Engineering, 1025 N. Broadway, Milwaukee, WI 53202

Abstract

The Milwaukee School of Engineering (MSOE) and the Additive Manufacturing (AM) community have an interest in expanding applications of AM and broadening market opportunities. Specific areas of interest include robotics and fully functional components/systems. MSOE has developed methods for streamlining the development and implementation of functional fluid power components/systems, such as Magnetic Resonance Imaging (fMRI) robotic surgery systems, rescue robotics, and customized form-fit orthotic and prosthetic devices, all of which have a high power-density and high efficiency with the use of fluid power. MSOE has defined several of these components and devices as solid state actuators (SSA) (single, multi-functional components made of diaphragms, bellows, springs etc.) or solid state actuator systems (SSAS). Prior work has already been done on integrated systems for robotic prototypes to help determine and improve workspaces, thus allowing designers to make practical design changes at a low cost. Implementing AM fluid power devices in industry has also been done, where applications largely include human-machine interaction and biomimetic or continuum robotics. However, most devices are made up of numerous components in assemblies. MSOE has made it possible for mechanisms to be fully functional as built and as a single entity. The implementation and development of SSAs and SSASs are discussed along with practical design considerations of integrated functional fluid power components.

1. Introduction

1.1. Purpose

The Authors are presently involved with "Project 2G: Fluid Power Surgery and Rehabilitation via Compact, Integrated Systems" through the Center for Compact and Efficient Fluid Power (CCEFP) funded by the National Science Foundation (NSF). Objectives of Project 2G include:

- Developing fluid power devices for use in an intense magnetic field e.g. MRI-machine.
- Using MRI imaging for feedback in surgical procedures to reduce invasiveness.
- Improve understanding of fluid power to enable compact precision machinery.
- Cylinders, valves, and sensors are no longer assembled as separate components in a machine but are manufactured simultaneously in a compact and integrated system.

The objective of manufacturing assemblies simultaneously stood out as an application of AM for MSOE and was the main motive for developing fully functional integrated fluid power systems via AM.
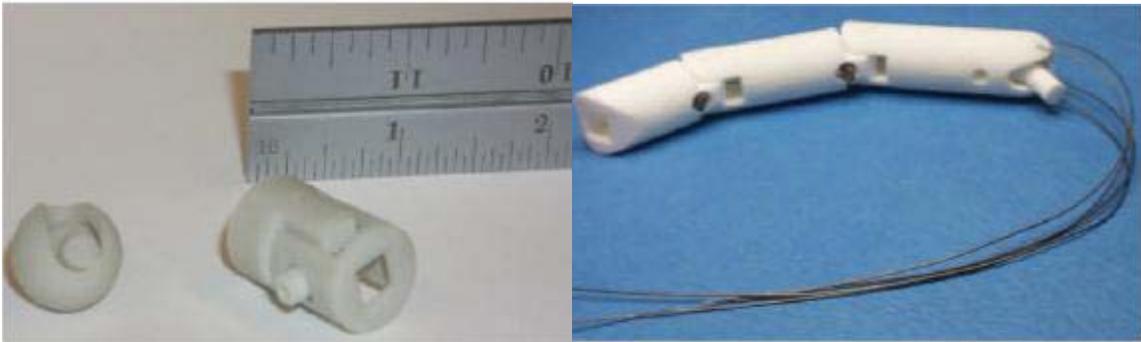
1.2.   Scope

MSOE's involvement with Project 2G and knowledge of AM applications with fully-functional fluid-power devices led to the initial ideation of several actuator concepts and systems. Technical challenges developing these mechanisms and machines were identified. MSOE's goal was to meet the challenges of Project 2G while addressing technical challenges associated with additively manufactured integrated functional fluid-power components/systems. The following challenges with AM and compact integrated fluid-power systems were addressed:

- Design for functionality in MRI environment.
- Modeling of precise motion.
- Challenges with mechanism design & recommendations.

Publications by other institutions have addressed some basic issues with integrated systems via AM, and those technical challenges are not in the scope of this published work. However, the integration of actuators in such integrated systems and methods for increasing the accuracy of integrated functional mechanisms was of a main focus.
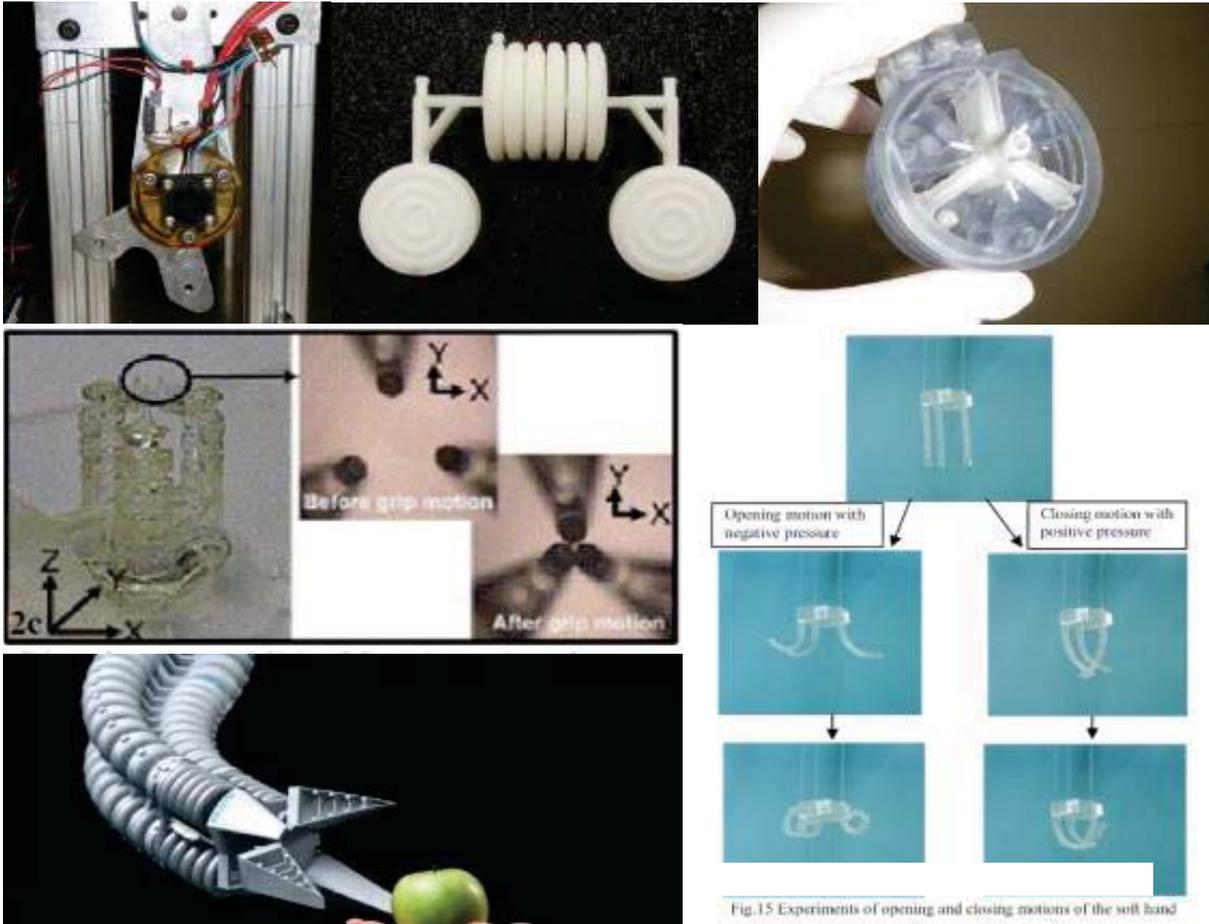
1.3.   Background

Using additive manufacturing for integrated mechanisms has several advantages over using conventional manufacturing methods including optimized multifunctional components that can use lattice structures to make components more efficient and lightweight [11, 14]. Previous work by other institutions with integrated mechanisms addressed technical challenges with tolerance errors as well as providing recommendations for integrated planar and spatial kinematic chains [4, 5, 12, 18]. Several examples of past mechanisms and joints of integrated mechanisms are illustrated in Figure 1.

Figure 1: Left) Modified spherical joint and universal joint Right) Integrated open loop chain (robotic finger actuated by SMA wires).

Research and development on diaphragm & bellows-based actuating elements was conducted by MSOE, Festo, and other institutions using different manufacturing processes [8, 10, 16, 17, 19]. Figure 2 illustrates a variety of pneumatic powered devices that are made with SLA, SLS, and silicone castings and hybrid combinations of 2 or more manufacturing processes [14, 15].

Figure 2: Examples of fluid power additively manufactured devices.

Limited literature is available addressing the technical challenges with the integration of fluid power actuators combined with pre-assembled integrated mechanisms. Integrated mechanisms and the use of AM bring rise to design limitations due to tolerances, controllability and stability of continuum-based actuators and mechanism configurations that result in joint binding and difficulties with freeing the mechanism.

These technical challenges implementing embedded mechanisms using AM led to the culmination of ideas to conceive Solid State Actuators (SSA) and Solid State Actuator Systems (SSASs). The Authors defined SSAs and SSASs as an actuator or actuating system that uses a

combination of elastic elements (e.g. diaphragms, bellows, springs), integrated fluid circuits, embedded joints/links, and is manufactured as a single, multi-component, functional system. The manufacturing can be done with no assembly and in a cost-effective manner using AM. This method also allows for multiple complex paths of actuation to be achieved from a single component or system (in addition to traditional linear and rotary actuation).

The development of SSAs and SSASs are presented herein including, modeling of SSAs, technical challenges encountered with a SSAS, case study of an integrated Gough-Stewart platform, recommendations for SSASs design, in addition to future work to be pursued on SSAs and integrated mechanisms.
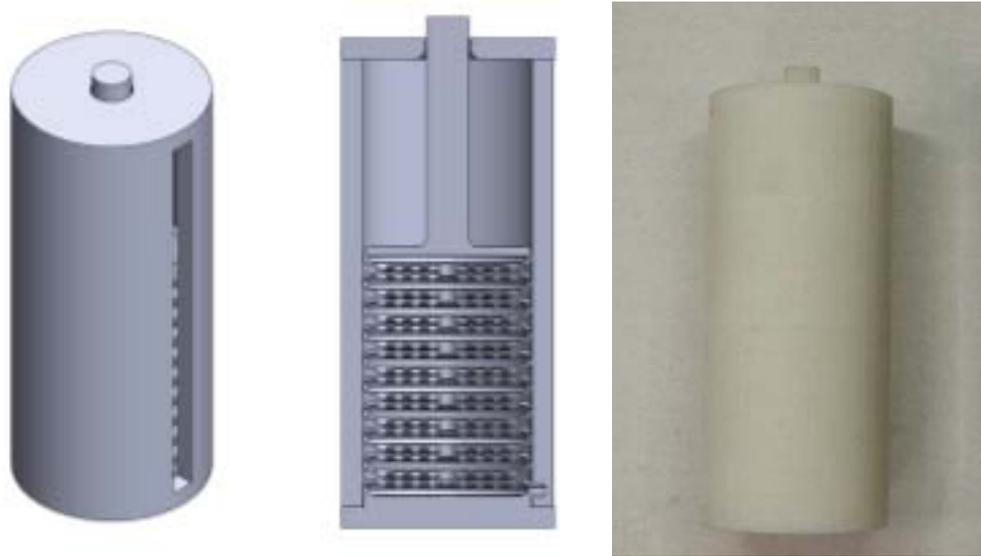
2. Actuator Development

2.1. Actuator Conceptualization

The conceptualization of SSAs culminated from the need for the aforementioned compact fluid power devices, whereby all components such as actuator, sensors, and valving are manufactured or "grown" in a fully-assembled form. Additive manufacturing was an obvious solution to the problem, as with laser sintering, one can create complex embedded components and mechanisms with moving parts. Traditional piston cylinder actuators were not feasible due to the variety of materials, surface finishes, and tolerances required for efficient and precise operation of a piston-cylinder actuator. A viable direction for an actuating device was to use a diaphragm or bellows type actuator. Some prior work with bellows based pneumatic actuators had been completed at MSOE and elsewhere with AM as well as conventional manufacturing methods.

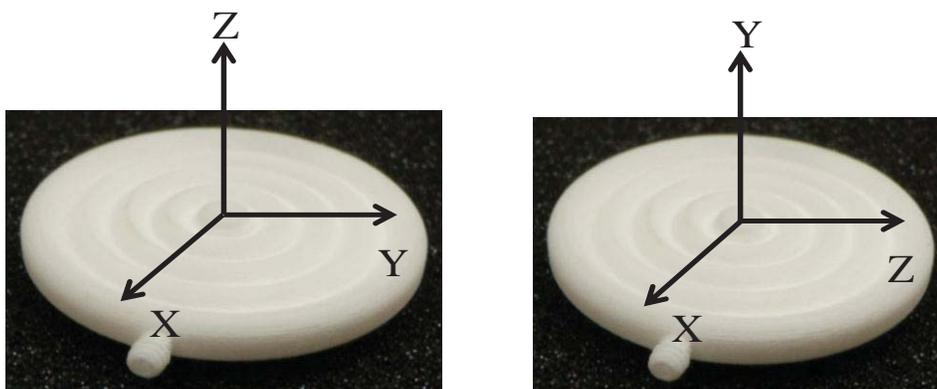**Figure 3: Bellows actuators designed and manufactured at MSOE.**

The embedded bellows type actuator was the most feasible type of actuation for development that could provide stable actuation, with reasonable forces and actuation strokes. An initial concept was synthesized knowing this, and with the added flexibility of AM, held the notion of providing complex curvilinear motion paths beyond linear and rotary motion. The first generation CAD and SLS SSA are depicted in Figure 4.

Figure 4: Initial concept actuator CAD and SLS SSA.

2.2. Modeling and Characterization

The initial modeling of the SSAs was done by determining the static and dynamic characteristics of the diaphragms used in the bellows type actuators first with experimental methods. Diaphragms were designed using a FEA software package and compared to experimental static displacement results using material properties obtained by Ramos-Grez [13]. After an initial design, experimental methods were used for characterizing the diaphragms performance. Corrugated diaphragms were designed for the SSA concept to provide linear deflection characteristics [6, 7]. The corrugated diaphragms used in the embedded bellows are depicted in two different build orientations in Figure 5.

Figure 5: Y and Z build orientations of corrugated diaphragms (2in. O.D.).

For the static modeling of the diaphragms, the standard linear spring model was used since most corrugated diaphragms exhibit linear characteristics. The stiffness of the diaphragm, the force exerted by the internal pressure, and the axial loading conditions determine the displacement of the diaphragm, which is defined in equation (1).

$$Y_0 = \frac{PA_a - L}{K_D} \tag{1}$$

Where P is the internal pressure, A_a is the active internal surface area of the diaphragm, L is the axial load on the diaphragm, and K_D is the stiffness of the diaphragm. However, when stacking diaphragms in a series as a bellows, the total stiffness of the bellows is lowered and governed by equation (2) [6].

$$K_B = \frac{1}{\sum_{i=1}^{n}\left(\frac{1}{K_D}\right)} \tag{2}$$

Where the stiffness of the bellows is the inverse of the inverse-summation of each diaphragm stiffness.

Using equation (1) and (2), the displacement can be predicted for diaphragm or bellows in a solid state actuator. Figure 6 and 7 illustrate the predicted displacements of the corrugated diaphragms illustrated in Figure 5 built in the Y and Z orientation, respectively.
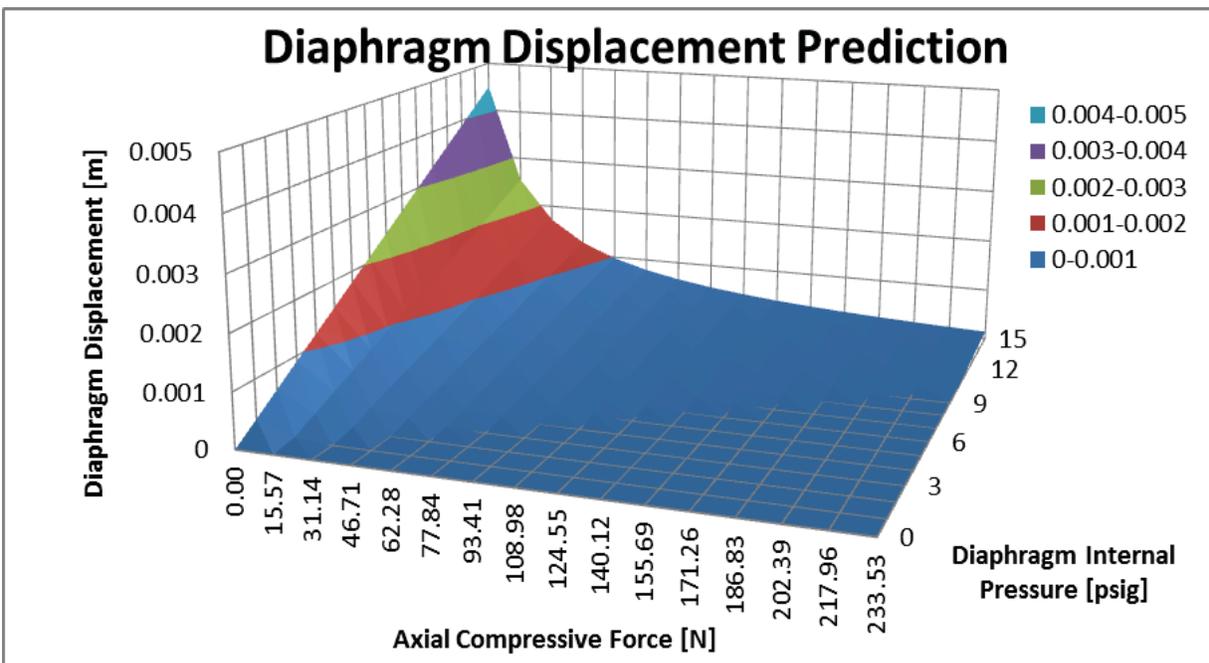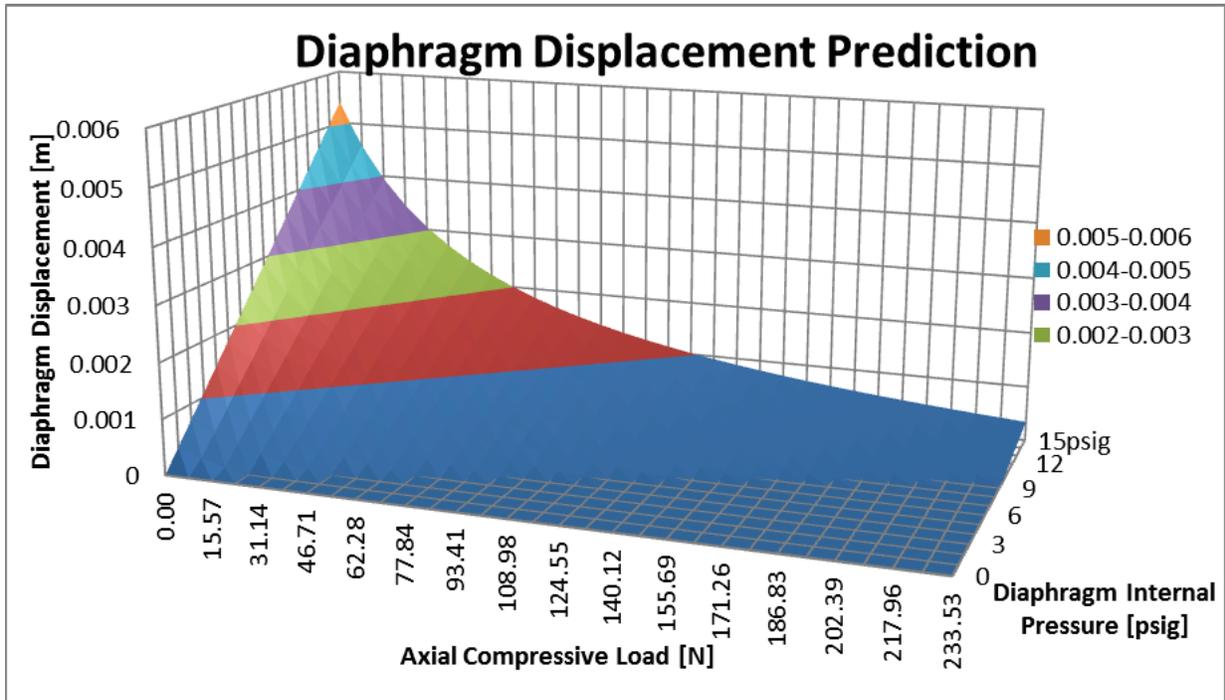

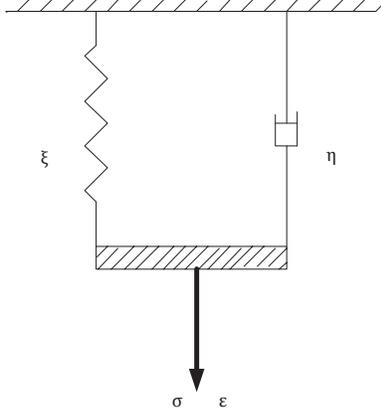**Figure 6: Y-orientation diaphragm displacement prediction.**

Figure 7: Z-orientation diaphragm displacement prediction.

Theoretically, the governing equation of displacement appears sound, however, due to the precision required for robotic surgery the uncertainty in the position is also required. The uncertainty in position of the diaphragm or bellows in an SSA is determined using equation (3).

$$\sigma_Y = \left[\left(\frac{A_a - L}{K}\right)^2 \sigma_P{}^2 + \left(\frac{P - L}{K}\right)^2 \sigma_{A_a}^2 + \left(\frac{PA_a}{K}\right)^2 \sigma_L^2 + (PA_a - L)^2 \left(\sqrt{\left(\sigma_{Y_0}^2 + m^2\sigma_P^2\right)}\right)^2\right]^{1/2} \quad (3)$$

Where σ_{Y_0}, is the uncertainty in displacement measurement to experimentally determine the diaphragms stiffness, m is the mass or force applied to the diaphragm to experimentally determine the diaphragms stiffness, σ_P is the uncertainty in pressure measurement, σ_L is the uncertainty in loading conditions on the bellows or diaphragm, and σ_{A_a} is the uncertainty in the effective internal surface area of the diaphragm.

For an accurate dynamic characterization of a diaphragm or bellows system, the Kelvin-Voigt viscoelastic model is used to portray the viscoelastic behavior the polyamide material being used where the free-body-diagram (FBD) of the Kelvin-Voigt model is illustrated below in Figure 8 [1, 3, 9].

Figure 8: Kelvin-Voigt viscoelastic FBD model.

The displacement also known as the macroscopic strain on the component and is defined in equation (4) as determined from the FBD as a function of time.

$$\varepsilon(t) = \frac{\sigma_o}{E} + \frac{\sigma_o}{\xi}\left[1 - e^{-\left(\frac{\xi}{\eta}\right)t}\right] \tag{4}$$

ξ and η are material constants that define the viscoelastic characteristics of the material i.e. creep [3].

The stress in the diaphragm causing the strain is a function of the internal pressure in the diaphragm and time. The dynamic behavior of the fluid is modeled by considering the choked flow across a solenoid valve using the sonic trans-conductance equation shown as equation (5) [15].

$$\frac{dP_2}{dt} = \frac{\gamma}{V}10CP_1\sqrt{1 - \left[\frac{\frac{P_2}{P_1} - b}{1 - b}\right]^2}\sqrt{\frac{298}{T}} \tag{5}$$
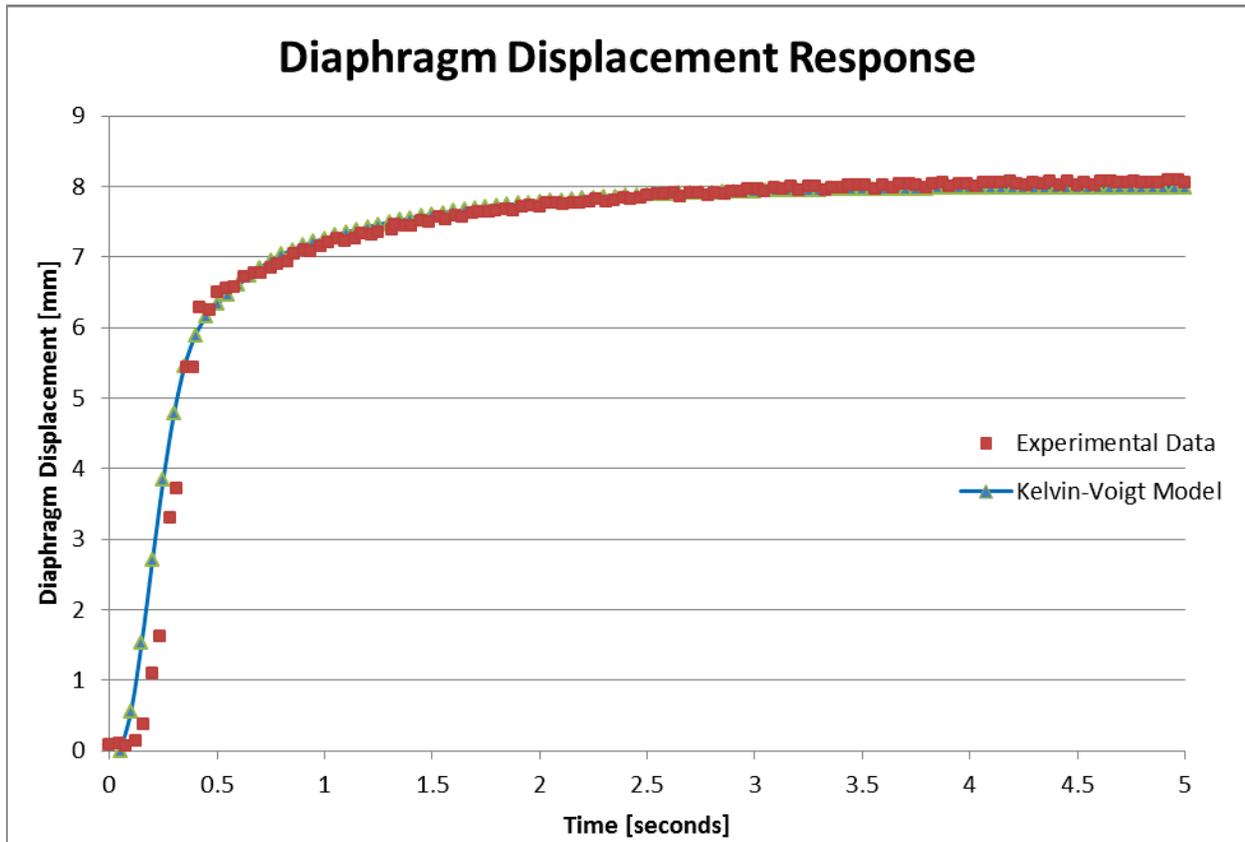
Where P_2 is the absolute downstream pressure over the valve, P_1 is the valve absolute upstream pressure, C is the sonic conductance constant, b is the critical pressure ratio, T is the temperature absolute, γ is the ration of constant-pressure specific heat to the constant-volume specific heat, and V is the volume of downstream of the valve. The solution of equation (5) using Euler's method is illustrated below in equation (6), where step size must be very small, around one hundredth of a second or less.

$$P_2(t) = P_{o,2} + \frac{\gamma}{V}10CP_1\sqrt{1 - \left[\frac{\frac{P_{o,2}}{P_1} - b}{1 - b}\right]^2}\sqrt{\frac{298}{T}}(t_1 - t_0) \tag{6}$$

Combining equation (4) and (6) we have equation (7)

$$\varepsilon(t) = \frac{\sigma(P(t))}{E} + \frac{\sigma(P(t))}{\xi}\left[1 - e^{(\xi/\eta)t}\right]$$ (7)

Using equation (7) and running dynamic test trials, the viscoelastic constants can be determined by using the method of least-of-squares-fit [2]. Figure 9 depicts some early experimental results and curve fitting conducted on Z-oriented diaphragms.
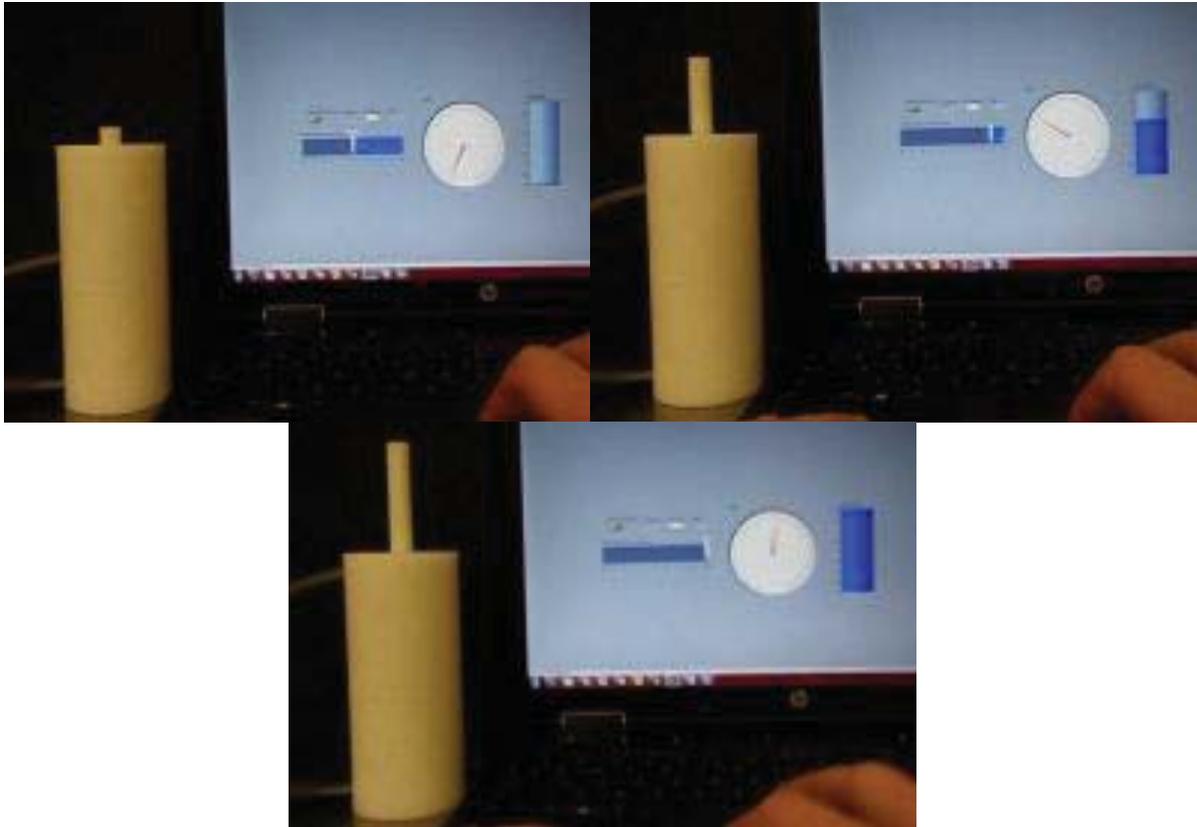

Figure 9: Diaphragm displacement response experimental and curve fit results.

Using experimental methods to determine stiffness and viscoelastic coefficients is an effective method for diaphragm and actuator characterization on a case-by-case basis. The uncertainty in the materials and changes in sintering machine parameters with complex designs using AM are difficult to characterize using analytical methods [3, 7].

2.3. Testing of Characterization

After the first concept was built, validation of open-loop testing was conducted to validate accuracy of the diaphragm characterization. The orientation of the SSA built was in the

Z-orientation and the predicted positioning for the SSA was used from the data in Figure 7. The Z-oriented diaphragms were determined to have a stiffness of **K_D=43.35 kN/m**. Where the stiffness of the Z-oriented SSA was determined to be **K_B=4.81 kN/m.** Thus, from the characterization data, the relationships for position as a function of pressure could then be used in the control software and determine an estimated position of the actuator rod end. Figure 10 illustrates the open loop control and position estimation testing, where the bar meter on the right hand side of each figure is the estimated actuator position.

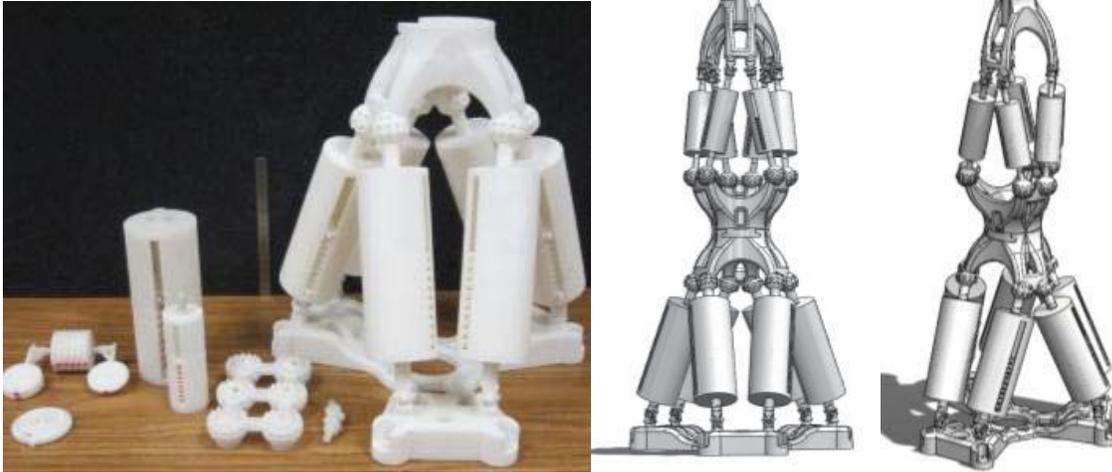**Figure 10: SSA open loop control and position estimation**.

Initial testing confirmed that the experiemental characterization methods used were effective in determining real-time actuator rod end position. Therefore, the characterization method could be implemented in Project 2G demonstrative mechanisms.

3. Actuator System Implementation

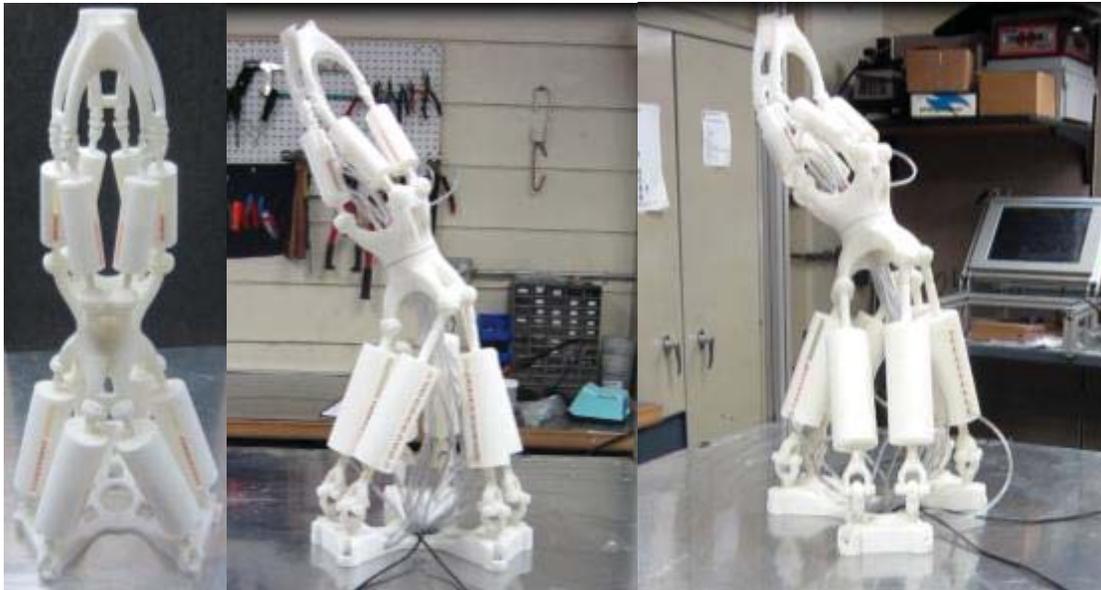#### 3.1. Case Study: Integrated Gough-Stewart Platform

To demonstrate the feasibility of SSAs in SSASs, a robotic system comprised of two Gough-Stewart platforms in a series was designed with the use of AM in mind. The tele-operated multi degree of freedom robotic system was designed such that all the components e.g. actuators, universal joints, spherical joints, and armatures, were built as one single entity. Considerations of

capable tolerances with embedded components using laser sintering were taken into account, but components were designed so clearances were minimized. The separate components, lower Gough-Stewart platform, SSAs and robotic system CAD are illustrated in Figure 11.

Figure 11: Seperate components, lower platform and CAD.

Implementation of the multi-level Gough-Stewart platform successfully demonstrated the feasibilty of SSASs, and the use of integrated systems with MRI compatable materials. Figure 12 illustrates the assembled robotic system and it's operation.
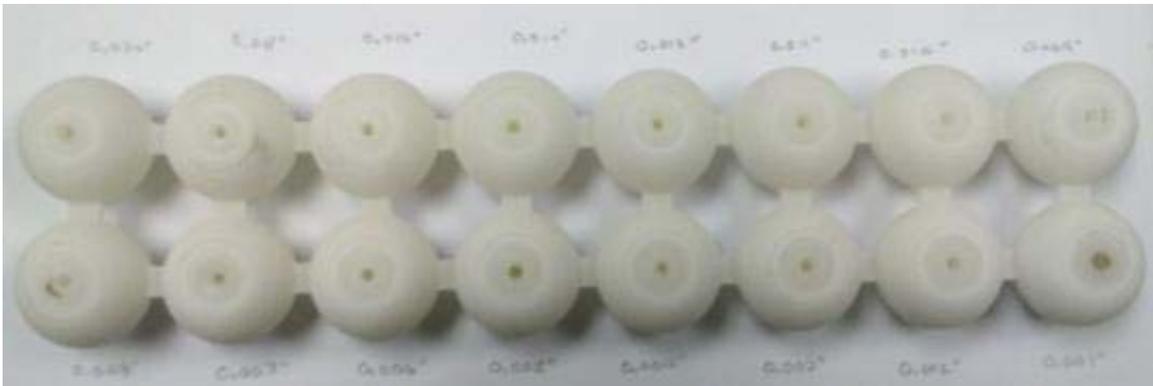

Figure 12: SSAS assembly and operation.

However, the build and implementation of the system did not go without the obstacle of new technical challenges. There were several factors that made the functionality of the integrated mechanism challenging. Factors included certain mechanism configurations that caused low

initial torque to free embedded joints in addition to joint and actuator powder and cake clean out difficulty due to the mechanism design. This provided qualitative insight to future fully functional embedded fluid power mechanism designs.
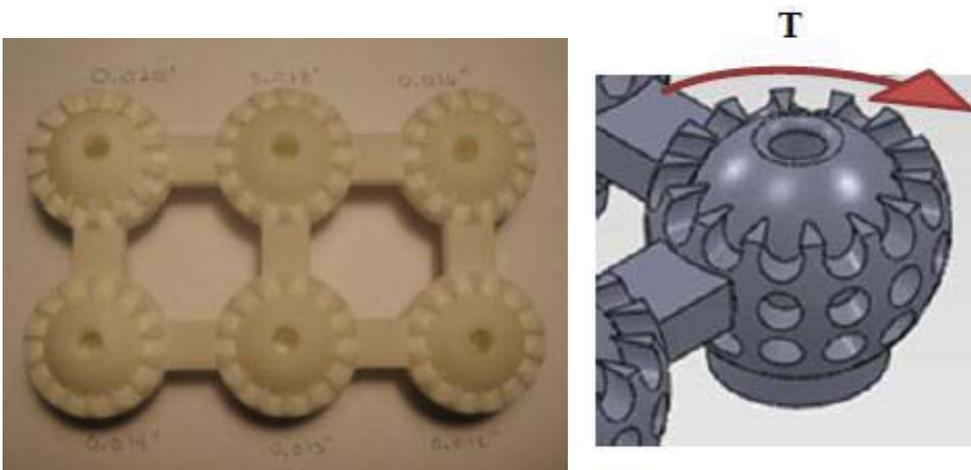
3.2. Design Recommendations for SLS Integrated Systems

Current limitations of SSASs are joint tolerances and joint cleanout for functionality. Joint tolerances are limited at best to approximately 0.3mm (0.012 in) with SLS nylon 12. With acceptable tolerances even larger than these specifications, problems with powder removal and part fusing can occur. For example, a small design experiment of spherical joints to determine the best achievable tolerances yielded unexpected results. Figure 13 illustrates a case were a ball could not be moved inside the socket due to the tightly packed un-sintered powder with clearances ranging from 0.001 inch to 0.020 inch.
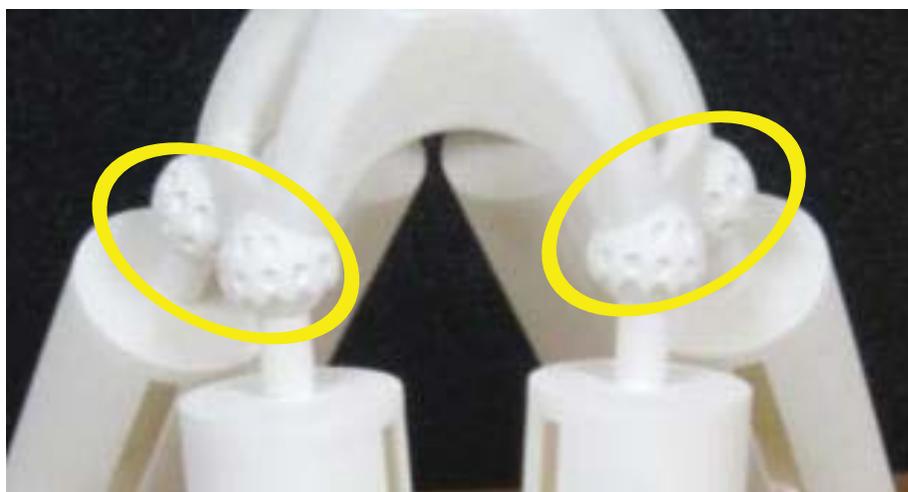

Figure 13: Fused spherical joints with varying tolerances.

Figure 14 shows another study done with spherical joints with a new porous socket design that allowed for better powder removal.

Figure 14: Modified socket spherical joint study.

The modified socket in the spherical joints allowed for the cleanout and functionality of the joint. However, there was an applied torque, T, required to free the joint as Figure 14 illustrates, regardless of how well the joint was cleaned out. This required break-out torque to free the joints, which was also observed in some pin joint designs, resulted in the lower Gough-Stewart platform being almost non-functional because the torque applied to the spherical joints through the acturators was not sufficient as Figure 15 highlights.

Figure 15: Lower Gough-Stewart platfrom problematic spherical joints.

This technical issue should be factored into future fully-functional fluid-power mechanism designs. The main emphasis is to configure the mechanism in such a way that the torque at the joints is maximized at their initial position or have the rate of angle change be maximized in the mechanism at that particular joint, if the joint is problematic. It is also hypothesized that the amount of surface area in contact with the embedded joint governs this breakout torque.

4. Conclusions

Implementing SSAs in SSASs illustrate possible functionality for applications such as MRI robotic surgery, customizable orthotic devices, and other applications with some improvement with joint tolerances. Using experimental methods of characterizing the performance of elastic elements in SSA development has aided predicting accurate open loop control and future closed loop control schemes. Limitations were also discovered in mechanism designs, where low initial torque at joints may cease functionality in the mechanism and this must be considered in SSAS design. Mechanical configurations should maximize the rate of angle change in their initial mechanical configurations to overcome breakout torque.

4.1. Future work

Future work involves improving the precision of the SSAs and determining quantifiable metrics in joint break out torque so designs can be more optimized and take full advantage of AM for SSASs.

4.2. Acknowledgements

5. References

[1]   **Brostow, W, & Corneliussen, R.** (1986). "Failure of plastics," New York: Macmillian Publishing Co.

[2]   **Chapra, S, C., S, Canale, R, & P., R.** (2009). "Numerical methods for engineers," McGraw-Hill ScienceEngineeringMath.

[3]   **Crawford, R.J.** (1998). "Plastics engineering," Elsevier.

[4]   **De Laurentis, Kathryn J., Mavroidis, Constantinos (2002). "**Procedure For Rapid Fabrication Of Non-Assembly Mechanisms With Embedded Components," Proceedings of 2002 Design Engineering Technical Conference. Montreal, Canada: ASME.

[5]   **De Laurentis, Kathryn J., Mavroidis, Constantinos (2004).** "Rapid fabrication of a non-assembly robotic hand with embedded components," Assembly Automation, Vol. 24 Iss: 4 pp. 394 – 405

[6]   **Di Giovanni, Mario.** (1982). "Flat and Corrugated Diaphragm Design Handbook," New York: Marcel Dekker Inc.

[7]   **Feidos'ev, V.I.** (1966). "Elastic elements of intruments," Jerusalem, Israel: Israel program for scientific traslations.

[8]   **Festo.** (2011, April). "Bionic Handling Assistant," http://www.festo.com/net/SupportPortal/Downloads/42050/Brosch_BHA_en_RZ_310311_lo_einzel.pdf

[9]   **Harper, C.** (1992). "Handbook of plastics, elastomers and composites," McGraw Hill Companies.

[10]   **Konishi, S, Nokata, M, Jeong, O, Kasuda, S, & Sakakibara, T.** (2006). "Pneumatic micro hand and miniaturized parallel link robot for micro manipulation robot

system," Proceedings of the Proceedings of the 2006 ieee international conference on robotics and automation (pp. 1036-1041). Orlando: IEEE.

[11]   **Kumar, N.** (2011, July 28). "10 questions for robotics engineer: Lonnie Love," Retrieved from http://www.ornl.gov/sci/ees/mssed/news.shtml#news711c

[12]   **Rajagopalan, S., Cutkosky, M. (1998).** "Tolerance Representation For Mechanism Assemblies In Layered Manufacturing," Proceedings of the 1998 Design Engineering Technical Conference. Atlanta, GA: ASME.

[13]   **Ramos-Grez, J, Amado-Becker, A, Yanez, M, Vargas, Y, & Gaete, L.** (2008). "Elastic tensor stiffness coefficients for sls nylon 12 under different degrees of densification as measured by ultrasonic technique," Rapid Prototyping Journal, 14(5), 260-270.

[14]   **Remmers, R, Gervasi, V, & Cook, D.** (2010). "Custom, integrated, pneumatic, rotary actuator for an active ankle-foot orthosis," Proceedings of the Solid freeform fabrication symposium (pp.816-827).

[15]   **Remmers**. (2010). "Fluid Power Actuator for use in Active Anke Foot Orthotics," MSOE Engineering Capstone Report. (pp 20-22).

[16]   **Suzumori, K, Endo, S, Kanda, T, Kato, N, & Suzuki, H.** (2007). "A bending pneumatic rubber actuator realizing soft-bodied manta swimming robot," Proceedings of the 2007 ieee international conference on robotics and automation (pp. 4975-4980). Rome, Italy: IEEE.

[17]   **Wakimoto, S, Ogura, K, & Suzumori, K.** (2009). "Miniature soft hand with curling rubber pneumatic actuators," IEEE International Conference on Robotics and Automation, 556-561.

[18]   **Won, Jey, DeLaurentis, Kathryn J., Mavroidis, Constantinos (2000).** "Fabrication Of A Robotic Hand Using Rapid Prototyping," Proceedings of 26th Biennial Mechanisms and Robotics Conference. Baltimore, Maryland: ASME.

[19]   **Zientarski, Sara** (15 April 2010). "Additive Manufacturing of Fully Functional Fluid PowerComponents," Proc. NCUR 2010.